Interdiffusion, Growth Mechanisms, and Critical Currents in $YBa_2Cu_3O_{7-x}/PrBa_2Cu_3O_{7-x}$ Superlattices

S. J. Pennycook, M. F. Chisholm, D. E. Jesson, D. P. Norton, D. H. Lowndes, R. Feenstra, and H. R. Kerchner

Solid State Division, Oak Ridge National Laboratory, Oak Ridge, Tennessee 37831-6030

J. O. Thomson

The University of Tennessee, Department of Physics and Astronomy, Knoxville, Tennessee 37996-1200

(Received 4 April 1991)

Z-contrast electron microscopy demonstrates that interdiffusion is not affecting the resistive transitions observed in $M \times N$ $YBa_2Cu_3O_{7-x}/PrBa_2Cu_3O_{7-x}$ superlattices. At moderate supersaturations, island growth is observed, the islands comprising one Ba-Y-Ba structural unit in height terminated at the Cu-chain plane, having sides 20–30 nm long along [100] and [010]. The associated gradual roughening of the growing surface has no apparent effect on critical currents for $M \geq 2$, the temperature and field dependence being comparable to that of a film.

PACS numbers: 74.70.Vy, 61.16.Di, 74.60.Mj

Superlattices of $YBa_2Cu_3O_{7-x}/PrBa_2Cu_3O_{7-x}$ (denoted as YBCO/PBCO) show strong and systematic variations in their transport properties with both layer thicknesses [1–3]. There is considerable current interest in such data since it provides a sensitive test for any theory concerning the nature and origin of superconductivity in the high-T_c materials [4–8]. The crucial question for any such interpretation, however, concerns the compositional integrity of the individual layers. Studies of the alloy $Y_{1-y}Pr_yBa_2Cu_3O_{7-x}$ have shown that T_c reduces rapidly with increasing Pr content, becoming semiconducting at $y \geq 0.5$ [9]. Since it is perfectly possible to have a strong compositional modulation, as seen, for example, via satellite peaks in x-ray diffraction, but to have a substantial Pr concentration within the YBCO layers, this key question remains at present completely unaddressed.

In principle, it is possible to analyze the envelope of the satellite diffraction peaks to obtain information on the shape of the compositional modulation, but this would naturally represent an average measurement over a substantial lateral area and the entire film thickness. It could well convey a misleading picture of the actual situation, as can be recognized immediately from Fig. 1, which shows significant undulations in the layers of a nominally 1×8 superlattice. The micrograph shows 11.7-Å c-axis lattice fringes, the fainter contrast corresponding to higher Y content. Because of the undulations, we must consider separately the question of interdiffusion and the possible effects of the waviness. We can, in fact, deduce from this image that significant interdiffusion must be restricted to a distance of the order of a single unit cell, but again this sensitivity does not come close to excluding interdiffusion as a significant factor in the observed superlattice transport properties.

In this paper, we utilize the recently developed Z-contrast technique [10] for high-resolution electron microscopy to answer this important question. In addition, since each individual YBCO layer acts as a marker, replicating the growth surface below, we obtain a remarkably detailed picture of the surface morphology and the growth mechanism itself. The Z-contrast technique combines atomic-resolution imaging with compositional sensitivity, which has not been achieved in this system using conventional phase-contrast techniques based on Fourier reconstruction. In the Z-contrast method, a finely focused electron probe is scanned across the sample while the integrated intensity scattered through large angles (75–150 mrad) is used to form an image. For a crystal in a planar or zone-axis orientation, the image maps out the planar or columnar scattering power with the resolution of the probe. For a sufficiently fine probe [2.2 Å in our VG Microscopes HB501UX scanning transmission electron microscope (STEM)], the atomic planes or columns are resolved, their respective intensity being dominated by the nearly Z^2 dependence of the high-angle scattering cross section, Z being the atomic number. No interference effects such as contrast reversals or Fresnel fringes occur so that Y ($Z=39$) is clearly distinguishable from Pr ($Z=59$), appearing respectively fainter and brighter than Ba ($Z=56$). The image contrast is dominated by the scattering cross sections [11], dynamical

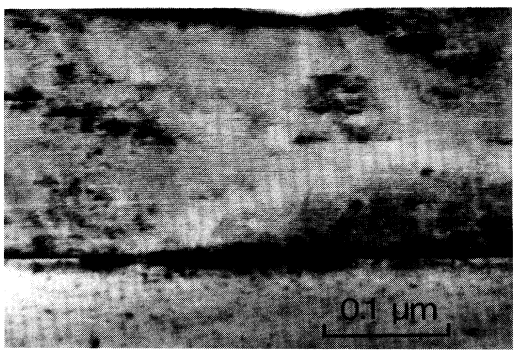

FIG. 1. Cross-section transmission electron micrograph of a 1×8 YBCO/PBCO superlattice. The 11.7-Å lattice fringes clearly indicate undulations in the layers.

© 1991 The American Physical Society

effects being second order compared to changes in concentration. Image statistics therefore set the minimum detectable Pr content in individual $Y_{1-y}Pr_y$ columns, typically to 10% for a sample 10–20 nm thick. Averaging over several columns will of course increase our sensitivity.

The growth and transport properties of our $M \times N$ YBCO/PBCO superlattices have been reported in detail elsewhere [3]. Briefly, the superlattices were grown by laser ablation using a KrF (248 nm) laser at 1.1 Hz in 200 mTorr O_2, providing an average deposition rate of approximately 1 $Å s^{-1}$. The heater temperature was maintained at 730 °C; the substrate temperature is estimated to be 670 °C. Growth was interrupted for approximately 20 s each time the ablation targets were interchanged.

Figure 2(a) shows a Z-contrast image obtained from the 1×8 superlattice shown in Fig. 1. In this low-magnification view, the three cation planes per cell are just resolved, each cell being separated by a dark line representing the Cu-chain planes. It is quite clear from this image that the Y is confined to a single unit cell which is seen to jump occasionally by one unit cell. This represents the microscope origin of the apparent waviness in Fig. 1. In Fig. 2(b), we show an interface in a nominally 3×5 superlattice which clearly demonstrates that no significant diffusion of Pr has occurred into the Y cells. The slight increase in intensity toward the top of the image is due to increasing sample thickness. Perhaps the best evidence that interdiffusion is insignificant is the observation of an abrupt interface step at the lower interface. The composition changes from YBCO to PBCO within a single lattice parameter in the a-b plane. Since diffusion within this plane is substantially faster than diffusion along the c axis, this provides convincing evidence that interdiffusion cannot be significantly affecting the measured transport properties of these superlattices.

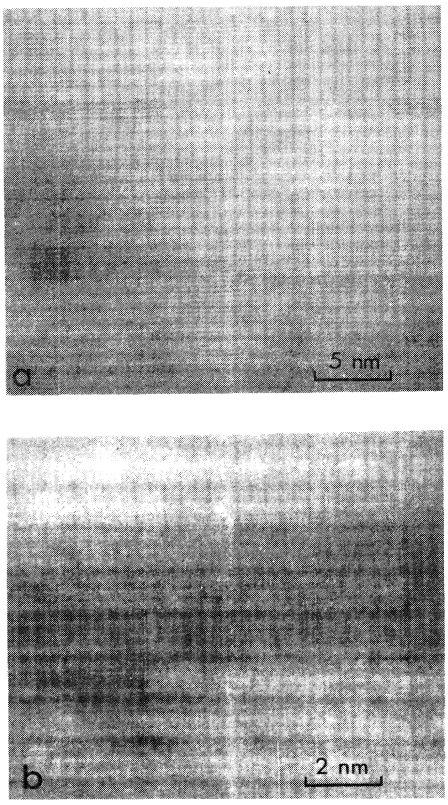

FIG. 2. (a) Z-contrast STEM image of the 1×8 superlattice showing YBCO layers (dark) one unit cell thick, jumping occasionally by one unit cell along the c axis. (b) Interface step in a 3×5 superlattice showing compositional abruptness of the order of one lattice parameter in the a-b plane.

We now turn to the question of the growth mechanism. The roughening of the growth surface evident from the undulations in Fig. 1 is associated with the sequential nucleation and coalescence of islands. A two-dimensional, terrace sweeping growth mode would maintain a constant surface morphology. The single-cell YBCO layers allow a direct view of the island morphology and arrangements, and from images such as Fig. 2(a), we determine a lateral island dimension of 24 ± 15 nm. The observation in Fig. 2(b) of an abrupt interface step, besides ruling out interdiffusion, implies that the island edge must lie parallel to the [100] or [010] electron-beam direction for practically the entire film thickness (estimated at 10–20 nm in this region). Since growth occurs in the tetragonal phase [12], we do not expect (and have seen no evidence for) any anisotropy within the a-b plane. No structural defects occur on island coalescence, for example, the $c/3$ stacking faults seen with lower growth temperatures [13], which implies that the height of the islands must be an integral number of unit cells, and that the growth surface must lie at a mirror plane, either the Cu-chain plane or the Y/Pr plane.

From Fig. 2(a), we see clearly that the preferred island height is a single unit cell, and that substantial completion of the layer occurs before nucleation of the next layer. This is in complete accord with the recent observation of clear oscillations in reflection high-energy electron diffraction during continuous deposition of YBCO, in which the period of oscillation corresponded to c [14]. It is also entirely consistent with the gradual roughening evident in Fig. 1, which eventually builds up to the large-scale islands observed by scanning tunneling microscopy [15].

To answer the important remaining question of which plane terminates the island, we turn to what can be considered the reverse of the growth process, amorphization, induced via ion implantation. Figure 3 shows the amorphous/crystal interface produced as a result of room-temperature implantation of oxygen (3×15 cm^{-2}, 40 keV) into a laser-ablated film of YBCO. Although end-of-range damage is clearly present in the crystalline region, there is a remarkable tendency for the crystal to terminate at the Cu-chain plane, with the result that, again,

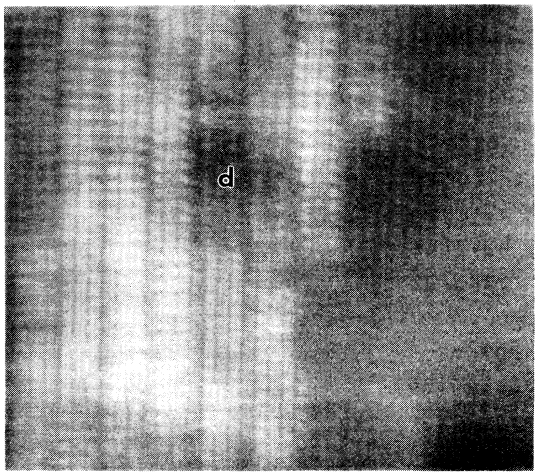

FIG. 3. The amorphous/crystal interface in a $c\perp$ ion-implanted YBCO film is located at the Cu-chain plane, and jumps frequently by one unit cell. End-of-range damage (marked d) is visible in the crystal.

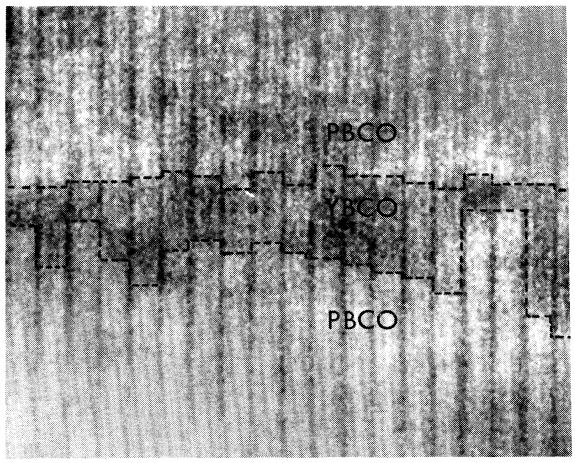

FIG. 4. Z-contrast image from a thin region of a 4×16 $a\perp$ superlattice showing considerable atomic-scale interfacial roughness.

we see interface steps a full unit cell in height. Clearly, at the end of the ion range, even amorphization occurs cell by cell, and so it should not be surprising that growth proceeds likewise. In fact, in all our Z-contrast observations of thin films and bulk materials, we see an overwhelming tendency to maintain a complete Ba-Y-Ba structural unit cell [13], both at low- and high-angle grain boundaries [16], and even at film/substrate interfaces, where substrate steps are forced to bunch in threes to accommodate complete Ba-Y-Ba blocks. As pointed out in Ref. [14], a complete unit cell is the minimum unit which can preserve stoichiometry and charge neutrality. Our observations highlight the remarkable structural stability of the Ba-Y-Ba (or Ba-Pr-Ba) block terminating at the Cu-chain plane [17]. In fact, it is only because of this property that it is possible to grow single-cell superlattices of the desired composition by laser ablation.

It is important to consider how the growth might vary as a function of supersaturation. The island size we observe is close to the minimum that can be achieved while maintaining $c\perp$ growth. At slightly higher supersaturations, it becomes kinetically favorable to switch to $a\perp$ growth, in which the fast crystal-growth direction is parallel to the film normal even though this is not the minimum-energy surface. Figure 4 shows a 4×16 $a\perp$ superlattice in which the interface shows considerable roughening at the atomic scale. This is to be expected since roughness now only adds {001} surfaces, which we know to have a particularly low surface (and interfacial) energy, so that there is little driving force toward smoothening. It would be of interest to increase the growth interruption between target changes in an attempt to reduce this surface roughness, since smooth $a\perp$ superlattices could provide a sensitive probe of the superconducting properties normal to the a-b plane. Note that this microscopic roughness precludes the buildup of macroscopic islands so that $a\perp$ films may often appear smoother [15]. Smoother $c\perp$ films could presumably be grown at lower supersaturations assuming, as seems likely, that misfit with the substrate is accommodated in the initial stages of film growth.

Finally, we consider possible effects of the island growth on superconducting properties. Provided no compositional variations occur and islands grow in the tetragonal phase, they will coalesce perfectly into larger grains. The island size, therefore, has no relevance for growth of a film. It is the relative alignment of the grains that is important for the film properties, which depends on other factors such as mismatch with the substrate, or the spacing and geometry of twins generated during the tetragonal-orthorhombic transition. In the case of the superlattices, as the width of an individual YBCO layer is reduced below the amplitude of its undulations, then we might expect the size of the islands to become significant. However, ac susceptibility measurements on a 2×4 superlattice (Fig. 5) show excellent critical-current behavior, comparable to that of a good thin film, indicating that the supercurrent is fully able to follow the imposed undulating path. Microscopically, the undulations comprise on average a one-unit-cell jump every island diameter so that a wavy $M\times N$ superlattice requires the current to transfer one cell along the c axis every $M-1$ island diameters. Our observations show that in YBCO, transfer along the c axis by one unit cell every 20–30 nm has no significant effect on the critical current. This also implies that a $2\times N$ superlattice would show no reduction in critical current for substrate misorientations of 2°–3°. Such "forgiving" behavior would not be expected for Bi- or Tl-based materials which appear significantly more two dimensional in their superconducting properties. Similarly, in $1\times N$ superlattices the average island overlap is zero, so that current transfer will be restricted to small

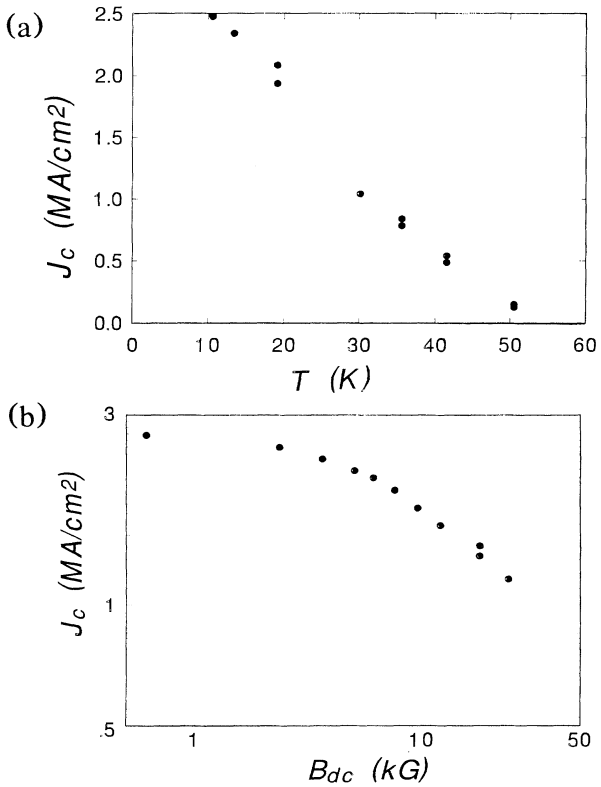

FIG. 5. Magnetic hysteresis measurements of critical currents in a 2×4 superlattice as a function of (a) temperature (for applied field $B=0$) and (b) applied field (at temperature 5 K).

"chance" areas of overlap at certain island edges, and we would anticipate greatly reduced critical currents with a clear weak-link behavior. Even in this case, however, at temperatures well below the mean-field critical temperature, the in-plane coherence length will be much less than the island size, and the resistive behavior is unlikely to be strongly affected. Therefore, the Kosterlitz-Thouless analysis of Ref. 8 would seem to be valid [18]. We should also point out that the interfacial steps are not the dominant pinning sites. Their density is independent of YBCO layer thickness, whereas there is experimental evidence that the pinning energy barrier increases linearly [19]. Far more likely to be dominant are oxygen vacancies or other point pins. Collective pinning theory yields a critical current proportional to the collective pinning energy barrier, which is proportional to the number of elementary pins per unit volume within a thin film [20].

In conclusion, Z-contrast imaging has demonstrated that interdiffusion is not a factor affecting the resistive transitions in YBCO/PBCO superlattices. At moderate supersaturations, $c\perp$ growth on $SrTiO_3$ occurs cell by cell through sequential nucleation and coalescence of islands, one complete Ba-Y-Ba structural unit high terminated at the Cu-chain plane, with sides 20–30 nm long along [100] and [010]. This intrinsic island growth leads to a gradual roughening of the growing surface and the eventual evolution of macroscopic islands. At higher supersaturations, $a\perp$ growth occurs with significant atomic-scale interfacial roughness. Amorphization via ion irradiation can also occur cell by cell.

We are grateful to M. Rasolt and J. D. Budai for helpful discussions. This work was sponsored by the Division of Materials Sciences, U.S. Department of Energy, under Contract No. DE-AC05-84OR21400 with Martin Marietta Energy Systems, Inc.

[1] J.-M. Triscone *et al.*, Phys. Rev. Lett. **64**, 804 (1990).
[2] Q. Li *et al.*, Phys. Rev. Lett. **64**, 3086 (1990).
[3] D. H. Lowndes, D. P. Norton, and J. D. Budai, Phys. Rev. Lett. **65**, 1160 (1990).
[4] A. Gold, Z. Phys. B **81**, 155 (1990).
[5] D. Ariosa and H. Beck, Phys. Rev. B **43**, 344 (1991).
[6] R. F. Wood, Phys. Rev. Lett. **66**, 829 (1991).
[7] J. Z. Wu, C. S. Ting, W. K. Chu, and X. X. Yao, Phys. Rev. B **44**, 411 (1991).
[8] M. Rasolt, T. Edis, and Z. Tesanovic, Phys. Rev. Lett. **66**, 2927 (1991).
[9] J. L. Peng *et al.*, Phys. Rev. B **40**, 4517 (1989).
[10] S. J. Pennycook and D. E. Jesson, Phys. Rev. Lett. **64**, 938 (1990).
[11] See, for example, S. J. Pennycook, S. D. Berger, and R. J. Culbertson, J. Microsc. **144**, 229 (1986).
[12] R. H. Hammond and R. Bormann, Physica (Amsterdam) **162-164C**, 703 (1989).
[13] S. J. Pennycook *et al.*, in *High Temperature Superconductors: Fundamental Properties and Novel Materials Processing,* edited by D. K. Christen, J. Narayan, and L. F. Schneemeyer, MRS Symposia Proceedings No. 169 (Materials Research Society, Pittsburgh, 1990), p. 765.
[14] T. Terashima *et al.*, Phys. Rev. Lett. **65**, 2684 (1990).
[15] D. P. Norton *et al.* (to be published).
[16] M. F. Chisholm and S. J. Pennycook, Nature (London) **351**, 47 (1991).
[17] Note that although we can unambiguously distinguish the observed Cu-chain plane termination from CuO_2 plane termination, this is achieved by imaging the Ba. At our present resolution, we have no information on the number or arrangement of the Cu atoms within this plane. Note also that our observed termination differs from that deduced from conventional high-resolution imaging. [H. W. Zandberger and G. van Tendeloo, in *High Temperature Superconductors: Relationships between Properties, Structure, and Solid-State Chemistry,* edited by J. B. Torrance *et al.*, MRS Symposia Proceedings No. 156 (Materials Research Society, Pittsburgh, 1989), p. 209.]
[18] It should also be noted that these superlattices are coherently strained, which may well have a significant influence on their transport properties [see A. Gupta *et al.*, Phys. Rev. Lett. **64**, 3191 (1990)].
[19] O. Brunner, L. Antognazza, J.-M. Triscone, L. Miéville, and Ø. Fischer (to be published).
[20] A. I. Larkin and Yu. N. Ovchinnuikiv, J. Low Temp. Phys. **34**, 409 (1979).

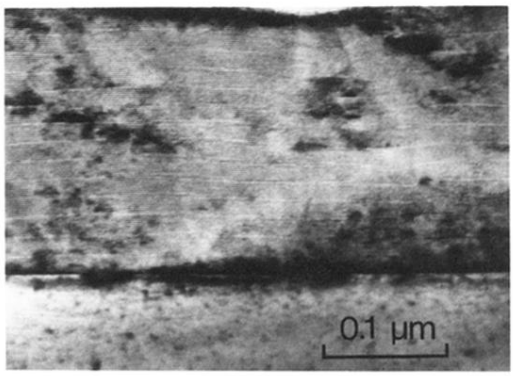

FIG. 1. Cross-section transmission electron micrograph of a 1×8 YBCO/PBCO superlattice. The 11.7-Å lattice fringes clearly indicate undulations in the layers.

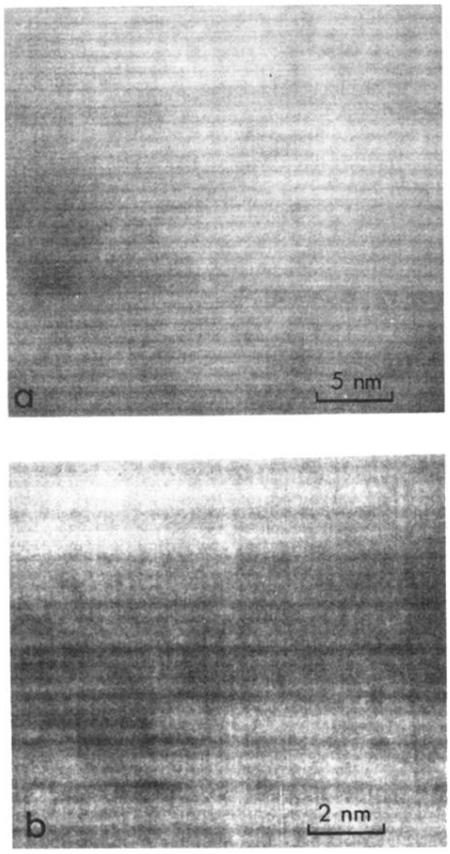

FIG. 2. (a) Z-contrast STEM image of the 1×8 superlattice showing YBCO layers (dark) one unit cell thick, jumping occasionally by one unit cell along the c axis. (b) Interface step in a 3×5 superlattice showing compositional abruptness of the order of one lattice parameter in the a-b plane.

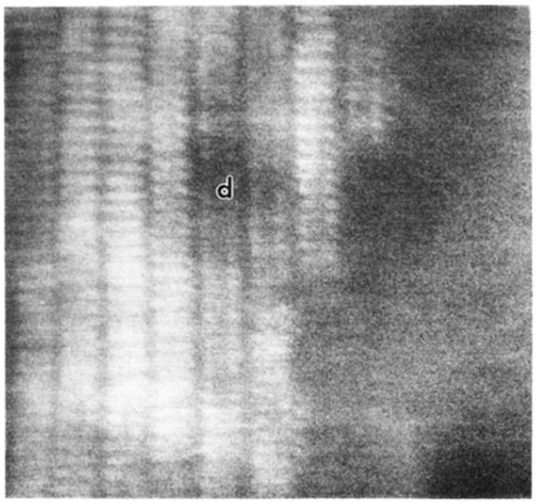

FIG. 3. The amorphous/crystal interface in a $c\perp$ ion-implanted YBCO film is located at the Cu-chain plane, and jumps frequently by one unit cell. End-of-range damage (marked *d*) is visible in the crystal.

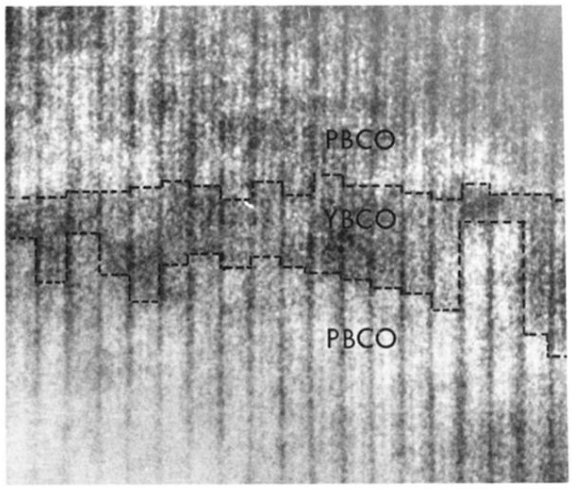

FIG. 4. Z-contrast image from a thin region of a 4×16 $a\perp$ superlattice showing considerable atomic-scale interfacial roughness.